Recent Geodynamics

THE 102–103° E GEODIVIDER IN THE MODERN LITHOSPHERE STRUCTURE OF CENTRAL ASIA

Yu. G. Gatinsky[1], T. V. Prokhorova[2], D. V. Rundquist[1]

[1] *V.I. Vernadsky State Geological Museum of RAS, Moscow, Russia*
[2] *Institute of Earthquake Prediction Theory and Mathematical Geophysics RAS, Moscow, Russia*

Abstract: A quasi-linear zone of noticeable geological and geophysical changes, which coincides approximately with 102–103° E meridians, is termed by the authors as "geodivider". Active submeridional faults are observed predominantly along the zone and coincide with its strike. Seismicity is most intensive in the central part of this zone, from the Lake Baikal to the Three Rivers Region at the Sino-Myanmar frontier. Transects with deep seismic sections and energy dissipation graphs show most sharply increasing seismic energy amounts and hypocenter depths in the western part of the geodivider which delimits (in the first approximation) the Central Asian and East Asian transitional zones between the North Eurasian, Indian and Pacific lithosphere plates. The transpression tectonic regime dominates west of the geodivider under the influence of the Hindustan Indentor pressure, and the transtension regime prevails east of it due to the Pacific subduction slab submergence and continuation. The regime change coincides with an abrupt increase in the crust thickness – from 35–40 km to 45–70 km – west of the geodivider, as reflected in the geophysical fields and metallogenic characteristics of the crust. The direction of *P*- and *S*-waves anisotropy together with the GPS data show decoupling layers of the crust and mantle in the southern part of the geodivider. According to our investigations, the 102–103° E geodivider is a regional geological-geophysical border that may be compared with the Tornquist Line, and, by its scale, with the Uralian and Appalachian fronts and some others large structures.

Key words: geodivider; lithosphere plate; block; active fault; transitional zone; crust and lithosphere thickness; seismicity; earthquake; magnitude; GPS data; displacement; geophysical field; deep seated anomaly in the crust and mantle; Central Asia

Геодивайдер 102–103° в.д. в современной структуре литосферы Центральной Азии

Ю. Г. Гатинский[1], Т. В. Прохорова[2], Д. В. Рундквист[1]

[1] *Государственный геологический музей им. В.И. Вернадского РАН, Москва, Россия*
[2] *Институт теории прогноза землетрясений и математической геофизики РАН, Москва, Россия*

Аннотация: Квазилинейная зона заметных геологических и геофизических изменений совпадает приблизительно с меридианами 102–103° в.д. Активные субмеридиональные разломы развиты в этой зоне, названной авторами геодивайдером 102–103° в.д. Наиболее интенсивная сейсмичность характеризует центральную часть геодивайдера от озера Байкал до региона Трех рек на границе Китая и Мианмар. Проведение трансектов с глубинными сейсмическими разрезами и графиками диссипации сейсмической энергии показывает преимущественно резкое возрастание объемов сейсмической энергии и глубины гипоцентров на западном крыле геодивайдера. Геодивайдер разделяет, в первом приближении, Центрально-Азиатскую и Восточно-Азиатскую транзитные зоны между Северо-Евразийской, Индийской и Тихоокеанской литосферными плитами. Тектонический режим транспрессии преобладает к западу от геодивайдера под влиянием давления Индостанского индентора, и режим транстенсии распространен к востоку от него, благодаря глубокому погружению и продолжению Тихоокеанского слэба. Смена режимов совпадает с резким увеличением мощности коры к западу от геодивайдера от 35–40 до 45–70 км, отражающимся в геофизических полях и коровых металлогенических характеристиках. Направление *P*- и *S*-волн анизотропии наряду с данными GPS показывает их несовпадение в различных слоях коры и мантии в южной части геодивайдера. По результатам наших исследований геодивайдер 102–103° в.д. представляет собой тип геолого-геофизической границы, сопоставимой с линией Торнквиста, по масштабу с Уральским и Аппалачским фронтами и с рядом других крупных структур.

Ключевые слова: геодивайдер; литосферная плита; блок; активный разлом; транзитная зона; мощность коры и литосферы; сейсмичность; землетрясение; магнитуда; данные GPS; смещение; геофизическое поле; глубинная аномалия в коре и мантии; Центральная Азия

1. Introduction

A quasi-linear zone of noticeable geological changes tracing across Eurasia clearly stands out on the Electronic Geodynamic Globe (http://earth.jscc.ru) created in the Vernadsky State Geological Museum in Moscow. The zone coincides approximately with 102–103° E meridians. Seismicity is intensive especially in the central part of this zone. Active faults are observed predominantly along the zone and coincide with its strike. We studied this zone in detail and, together with S. Cherkasov, named it "the 102–103° E geodivider" in our report at IGC 2004 in Florence [*Rundquist, 2004; Gatinsky et al., 2005*]. Later some geologists called it "the global meridional border structure" [*Sherman, 2015, 2016*] and "the North-South Tectonic Belt (NSTB)" [*Chang et al., 2015; Wang et al., 2015*]. The 102–103° E geodivider "neighbours" the VEBIRS Zone identified by geologists from Irkutsk in the 1970s [*Komarov et al., 1978*]. In this paper, we discuss the tectonic and geodynamic position of the geodivider, its seismicity, and its role in the modern structure of the continental lithosphere of Central Asia.

2. Problem statement

The 102–103° E geodivider is one of the most important tectonic structures in Central Asia. Throughout its extent it includes on the surface, especially in its central part, seismically active submeridional faults, and, in depth, sharp gradients of the crust and lithosphere thickness, gravimetric steps, changing velocities of *P*-waves in the upper mantle and developing low-velocity zones within the lower and middle crust. The geodivider delimits two main transitional zones, Central Asian (in the west) and East Asian. The former is located between North-Eurasian and Indian plates and characterized by the transpression regime with predomination thrusts and slips. The latter is located between the North Eurasian and Pacific plates and dominated by the transtension regime with extension structures [*Gatinsky et al., 2011*]. Our detail study of the geodivider and adjacent parts of transitional zones aimed at providing a fresh approach to interpreting the current regional geodynamics, the relations between the surface structures, their kinema-

tics and the deep anomalies, as well as clarifying the main causes of different regimes at the geodivider sides.

3. PROBLEM SOLVING METHODS

The following methods were effectively applied to solve the problem:

- Providing a more precise definition of the geodivider and the boundaries of the adjacent blocks on the basis of the Electronic Geodynamic Globe data; and the analysis of active faults and their hierarchy in the study area [*Xu, Deng, 1996; Sherman et al., 1999; Sherman, 2012, 2015; Trifonov et al., 2002; Seminsky, 2008; San'kov et al., 2015*];

- Analysis of the space-time distribution of earthquake epicenters and seismic tensors based on the data from the NEIC and CMT 2017 catalogs;

- Calculation of the releasing seismic energy volume using the formula from [*Kanamori, Anderson, 1975*], and computer simulation of its distribution patterns;

- Construction of the deep seismic sections based on the CMT data and the graphs of energy dissipation based on the NEIC data along the transects across the geodivider and the adjacent blocks;

- Analysis of the kinematics of the main lithospheric plates and blocks (http://itrf.ign.fr/ITRF_solutions/2014/), and comparison of these data with the actual displacement values along the active faults and the mechanisms recorded in the CMT 2017 catalog;

- Establishing a correlation between seismically active zones, geophysical fields and the results of deep seated lithosphere sounding.

4. ACTUAL DATA

Our study used the data from the NEIC and CMT 2017 catalogs, and the data on active faults, geophysical anomalies and deep seated structures, which was partly consolidated in [*Gatinsky, Prokhorova, 2014*].

5. CONNECTION OF THE GEODIVIDER WITH THE ADJACENT TECTONIC AND GEODYNAMIC STRUCTURES

In the extreme north, the 102–103° E geodivider coincides with the shelf margin of the Laptev Sea (Fig. 1). Further southwards it manifests itself in the eastern virgation and sharp northern deflection of Paleozoic folds and thrusts in the Severnaya Zemlya Archipelago and Taimyr. A buried Early Mesozoic rift traces the zone in the pre-Taimyr foredeep. Within the Siberian platform, the geodivider is marked by the west wing of the Anabar Anteclise and the buried

Riphean rift below the Tungus Syneclise. Further it nearly coincides with the southern jutting-out edge of the platform and squeezed fold structures in the East Sayan Belt.

In North Mongolia, the 102–103° E geodivider borders the centroclinal closure of the Hangay-Hentey Synclinorium [*San'kov et al., 2015*]. Further southward it coincides with the abruptly terminating and/or squeezed Paleozoic ophiolite belts. In Central and South Mongolia, a number of Cenozoic basalt fields are observed along the geodivider. The regional active fault bordering the western margin of the Amurian Block is located along the geodivider (Fig. 1). In North China, a virgation of Caledonian folds in Beishan and Qilian occurs eastward of the geodivider. Southward a wide virgation of Triassic folds takes place within the Indosinide field of Northwest Sichuan, where the folds go round the Songpan Massif – a buried fragment of the Yangtze Platform basement [*Tectonic Map…, 1999*].

The 102–103° E geodivider is most evidently detectable in South China. It distinctly coincides with the Kham Dian Axis that includes the metamorphic and magmatic rocks of the Late Proterozoic basement of the Yangtze Platform. In this region, active W-E striking faults, mostly sinistral slips including those accompanied by pull-apart basins, are observed along the geodivider. The geodivider is also marked by the sharp gradients of the upper mantle density, according to [*Li et al., 2011*]), as well as by a decrease in the *P*-wave velocity in the crust, which is detected by the Chinese geologists.

Within the Indochina Peninsula, the 102–103° E geodivider goes along the sharp west margin of the Indosinian Massif and coincides with some active eastward thrusts and slips of the sub-longitudinal strike [*Gatinsky*, *2005*]. Further southward, it is marked by transcurrent faults crossing the rift system of the Thailand Gulf, as well as by the Central Fold Belt of the Malay Peninsula and a flexure-like curve of the Cenozoic structural strike in South East Sumatra.

6. SEISMICITY OF THE GEODIVIDER AND THE ADJACENT BLOCKS

The central part of the 102–103° E geodivider from the southern termination of Lake Baikal to the Three Rivers Region at the Sino-Myanmar frontier (Fig. 2) is characterized by intensive seismicity in the Late Holocene and the current time. It coincides mainly with the block boundaries and interblock zones within the Central Asian and East Asian transitional zones discussed in detail in [*Gatinsky et al., 2009, 2011*].

Based on the data from the CMT and NEIC 2017 catalogs, we constructed transects with deep seismic
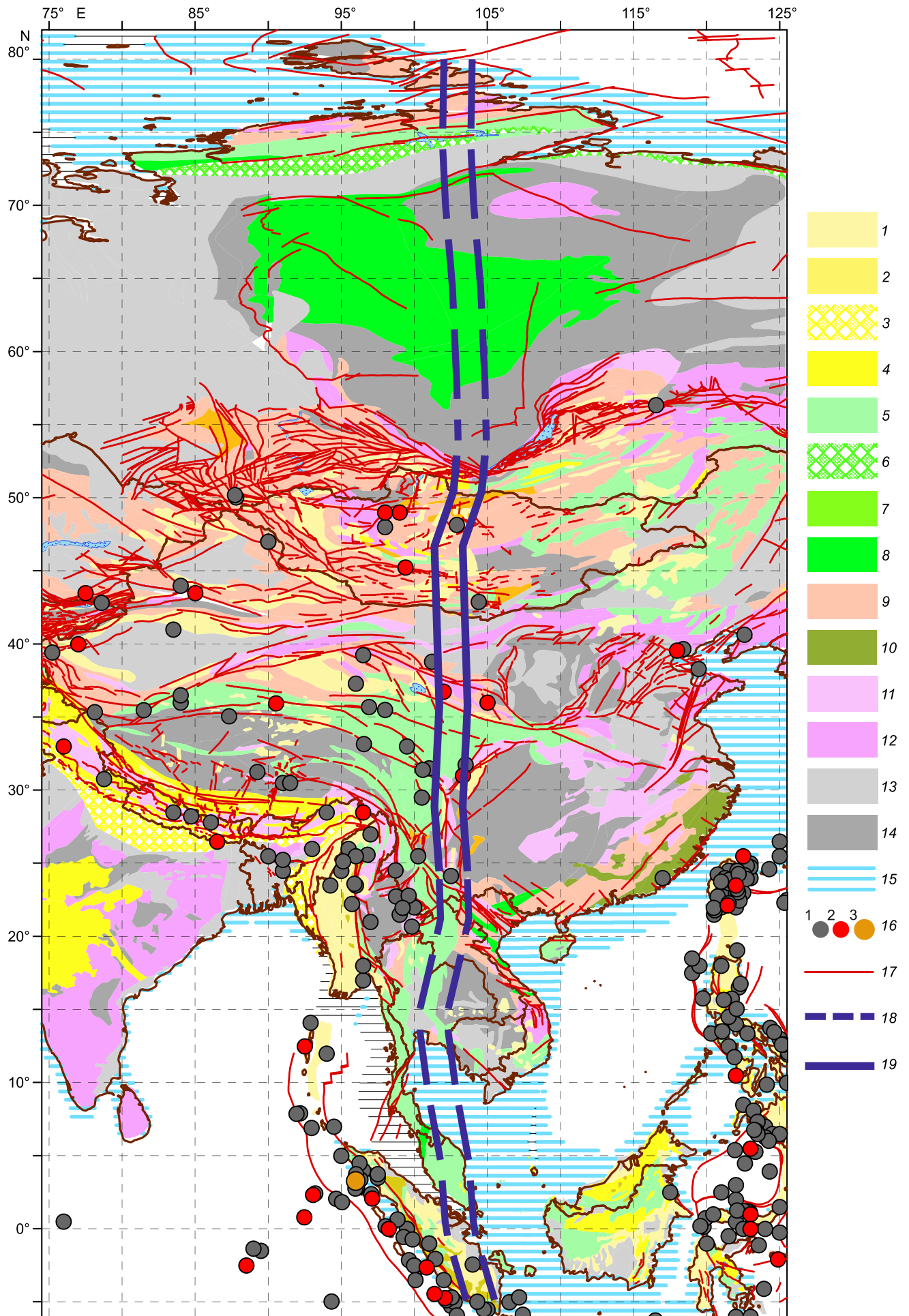
Fig. 1. The 102–103°E geodivider in the schematic tectonic map of Central Asia. The map is compiled on the basis of the Electronic Geodynamic Globe data (http://earth.jscc.ru).

1 – Cenozoic troughs; *2* – Cenozoic fold zones; *3* – Cenozoic Foredeep; *4* – Early Cenozoic trapps; *5* – Mesozoic fold zones; *6* – Mesozoic Foredeep; *7* – Mesozoic troughs; *8* – Early Mesozoic trapps; *9* – Late Paleozoic fold zones; *10* – Early Paleozoic fold zones; *11* – Late Precambrian fold zones; *12* – Early Precambrian basement; *13* – Mesozoic–Cenozoic platform cover; *14* – Paleozoic platform cover; *15* – current shelf; *16* – epicenters of the most intensive earthquakes after the NEIC 2017 data, and their magnitudes (1 – 7–8, 2 – 8–9, 3 – >9); *17* – active faults; *18* – northern and southern parts of the geodivider with not intensive seismicity; *19* – the central part of the geodivider with intensive seismicity. Note that the geodivider in the west borders the Anabar Anteclise and the Amurian block (the Amurian plate according to [*Zonenshain, Savostin, 1981*]).

Рис. 1. Геодивайдер 102–103° в.д. на тектонической схеме центральной части Азии, составленной на основе Электронного геодинамического глобуса (http://earth.jscc.ru).

1 – кайнозойские впадины; *2* – кайнозойские складчатые зоны; *3* – кайнозойские краевые прогибы; *4* – раннекайнозойские траппы; *5* – мезозойские складчатые зоны; *6* – мезозойские краевые прогибы; *7* – мезозойские впадины; *8* – раннемезозойские траппы; *9* – позднепалеозойские складчатые зоны; *10* – раннепалеозойские складчатые зоны; *11* – позднедокембрийские складчатые зоны; *12* – раннедокембрийский фундамент; *13* – мезозойско-кайнозойский платформенный чехол; *14* – палеозойский платформенный чехол; *15* – современный шельф; *16* – эпицентры наиболее интенсивных землетрясений с магнитудой: 1 – 7–8, 2 – 8–9, 3 – >9; *17* – активные разломы; *18* – северные и южные части геодивайдера с неинтенсивной сейсмичностью; *19* – центральная часть геодивайдера с интенсивной сейсмичностью. Следует обратить внимание, что геодивайдер ограничивает на западе Анабарскую антеклизу и Амурский блок (Амурскую плиту в другой интерпретации [*Zonenshain, Savostin, 1981*]).

sections and energy dissipation graphs, which allowed determining the earthquake mechanisms in hypocenters and the seismic energy volume distribution at the block boundaries. The seven transects cross the geodivider and the adjacent parts of the blocks (Fig. 2). Transect 1 (Fig. 3) shows that relatively shallow (8–12 km) left-lateral slips predominate in the east at the boundary of the Amurian and South Gobi blocks. Hypocenters with the same solution and several NE-trending thrusts are located in the west within the geodivider and west of it, but the releasing energy volume sharply increases there. Transect 2 (Fig. 4) shows that at the boundary between the Jartai and Qilian blocks, left-lateral slips coincide with its east part at the depth of 10 km and isolated one at 35 km. West within the geodivider, several NE-trending thrusts are observed with the same slips, especially at the depth (that increases to 43 km), and the seismic energy level is sharply increased in this zone.

Transect 3 crossing the West Qinlin and Qaidam blocks shows the same tendency with NE-trending thrusts in the west at the depth of 30–35 km and the increasing energy level (Fig. 5). However, inside the geodivider, the seismicity level is lower. One of the most informative is Transect 4 (Fig. 6) crossing the southern part of the Bayanhar Block in the region of the catastrophic Wenchuan earthquake (May 12, 2008, M 7.9). We discuss the regional kinematics below. Here it is worth noting that the 102–103° E geodivider in this region is marked by numerous right-lateral NW-trending slips and thrusts at the depth of 3–43 km at the SE border of the Bayanhar Block, wherein the seismic energy level is considerably increased. Further westward of the geodivider, numerous steady left-lateral slips at the depth of 2–50 km confirm the displacement direction along the SW block border [*Gatinsky et al., 2008*].

Transect 5 (Fig. 7) crosses the South East China, Kam Dian and North Tibet blocks. East of the geodivider, in South East China, rare NE-trending thrusts are observed at the depth of 10–33 km. Within the geodivider, the seismic energy level decreases. It sharply increases in the area west of the geodivider, wherein left-lateral and right-lateral slips dominate at the depth of 8–10 km, and extension hypocenters occur at the depth of 20–40 km. For the area further westward, the mechanism solutions show steady extension at the depth of 5–15 km, which is related to local submeridional rifts in Tibet. Within Transects 6 and 7 (Fig. 8 and 9), the geodivider is marked by a sharp growth of the energy level with the development of right-lateral and left-lateral slips as well as numerous extension structures at the depth of 0–50 km. In the west of the geodivider, the mechanism solutions correspond to the east-dipping slab of the West Burma subduction zone sinking to the depth of 140 km.

A sharp increase in the seismic energy quantity in the west wing of the geodivider is consistent with a higher mobility of blocks and the presence of anomalies in the lithosphere. Here we examine two regions of catastrophic seismic events – the SE part of the Bayanhar Block (its seismicity has been discussed above), and the NW side of the Amurian Block. The mechanism solutions show the left-lateral strike-slip displacement at the NE and SW boundaries of the Bayanhar Block (see Fig. 2 and 6) and suggest its clockwise rotation. As a result, the compression arises at the SE boundary of the block, wherein the disastrous M 7.9 Wenchuan
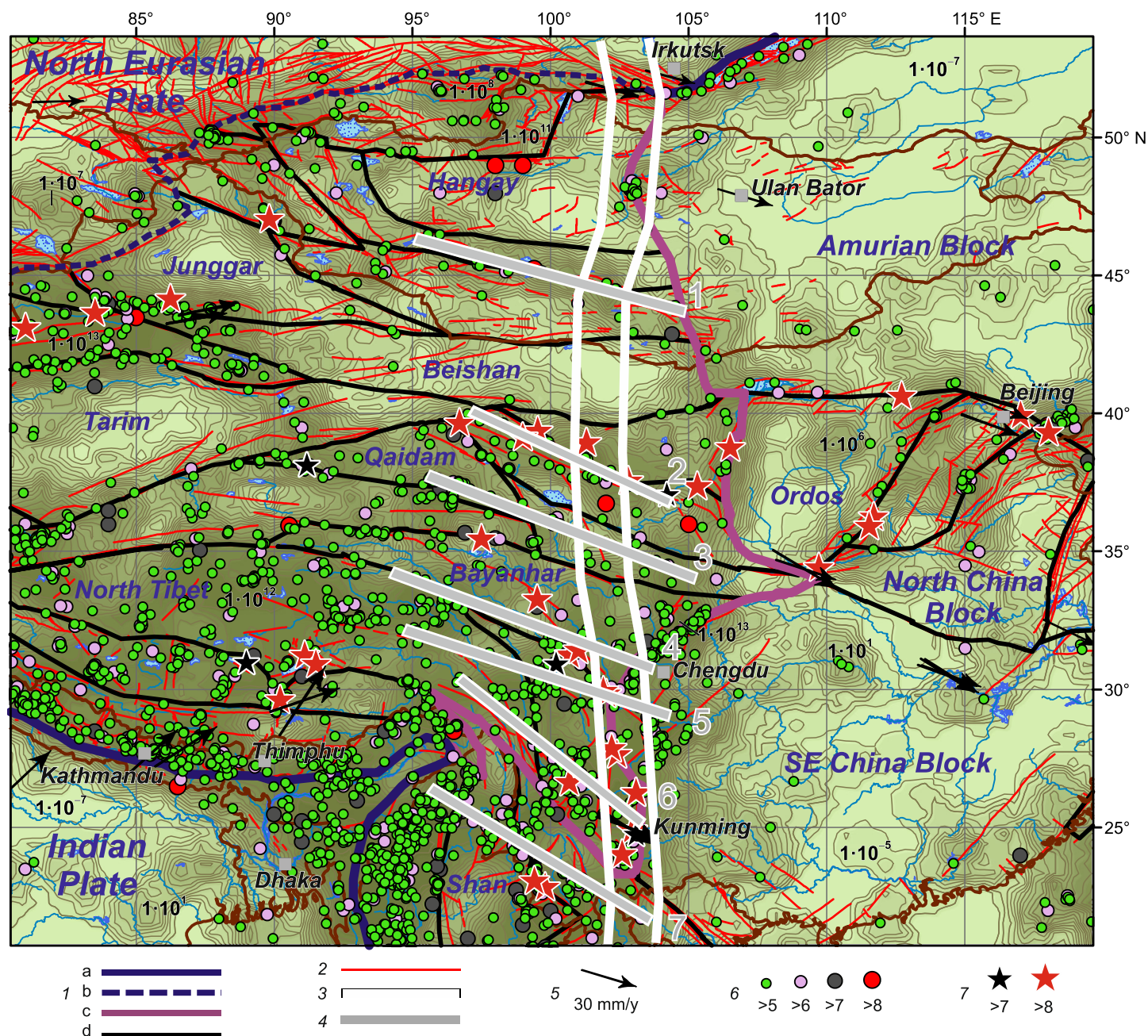
Fig. 2. The central part of the geodivider in the schematic geodynamic map of Central Asia.

1 – boundaries: a – between lithospheric plates, b – assumed, c – between the Central Asian and East Asian transitional zones, d – between blocks; *2* – active faults after [*Xu, Deng, 1996; Trifonov et al., 2002; Sherman et al., 1999; Sherman, 2012, 2015; Seminskii, 2008*]; *3* – borders of the geodivider; *4* – transect lines; *5* – computer-simulated ITRF vectors of horizontal displacement (*solutions/2014/ITRF2014.php*); *6* – epicenters and magnitudes of earthquakes (NEIC 2017 data); *7* – epicenters of historical earthquakes from the VIII to XIX century [*Xu, Deng, 1996*]. The intensity of olive-green colour corresponds to the seismic energy amount: each deeper colour reflects the seismic energy increase by 1×10^1 or 1×10^{-1} J. Some energy values are shown in the scheme in joules. Note the energy amount increasing within the geodivider and west of it nearly in all the areas, and the turn of ITRF vectors from the NE direction west of the geodivider to SE-east of it.

Рис. 2. Центральная часть геодивайдера на геодинамической схеме Центральной Азии.

1 – границы: а – литосферных плит, b – то же предполагаемые, с – между Центрально-Азиатской и Восточно-Азиатской транзитными зонами, d – блоков; *2* – активные разломы по [*Xu, Deng, 1996; Trifonov et al., 2002; Sherman et al., 1999; Sherman, 2012, 2015; Seminskii, 2008*]; *3* – границы геодивайдера; *4* – линии трансектов; *5* – экспериментальные ITRF векторы горизонтальных смещений (*solutions/2014/ITRF2014.php*); *6* – эпицентры землетрясений с определением магнитуд по данным NEIC 2017; *7* – эпицентры исторических землетрясений с VIII до XIX века [*Xu, Deng, 1996*]. Зелено-оливковые цвета отвечают объемам сейсмической энергии. Каждое увеличение интенсивности цвета совпадает с ростом энергии на 1×10^1 или 1×10^{-1} J. Отдельные объемы высвобождающейся энергии показаны на схеме в джоулях. Отмечается возрастание энергии в пределах геодивайдера и к западу от него почти на всех площадях так же как и на поворот векторов ITRF с СВ направления к западу от геодивайдера на ЮВ к востоку от него.
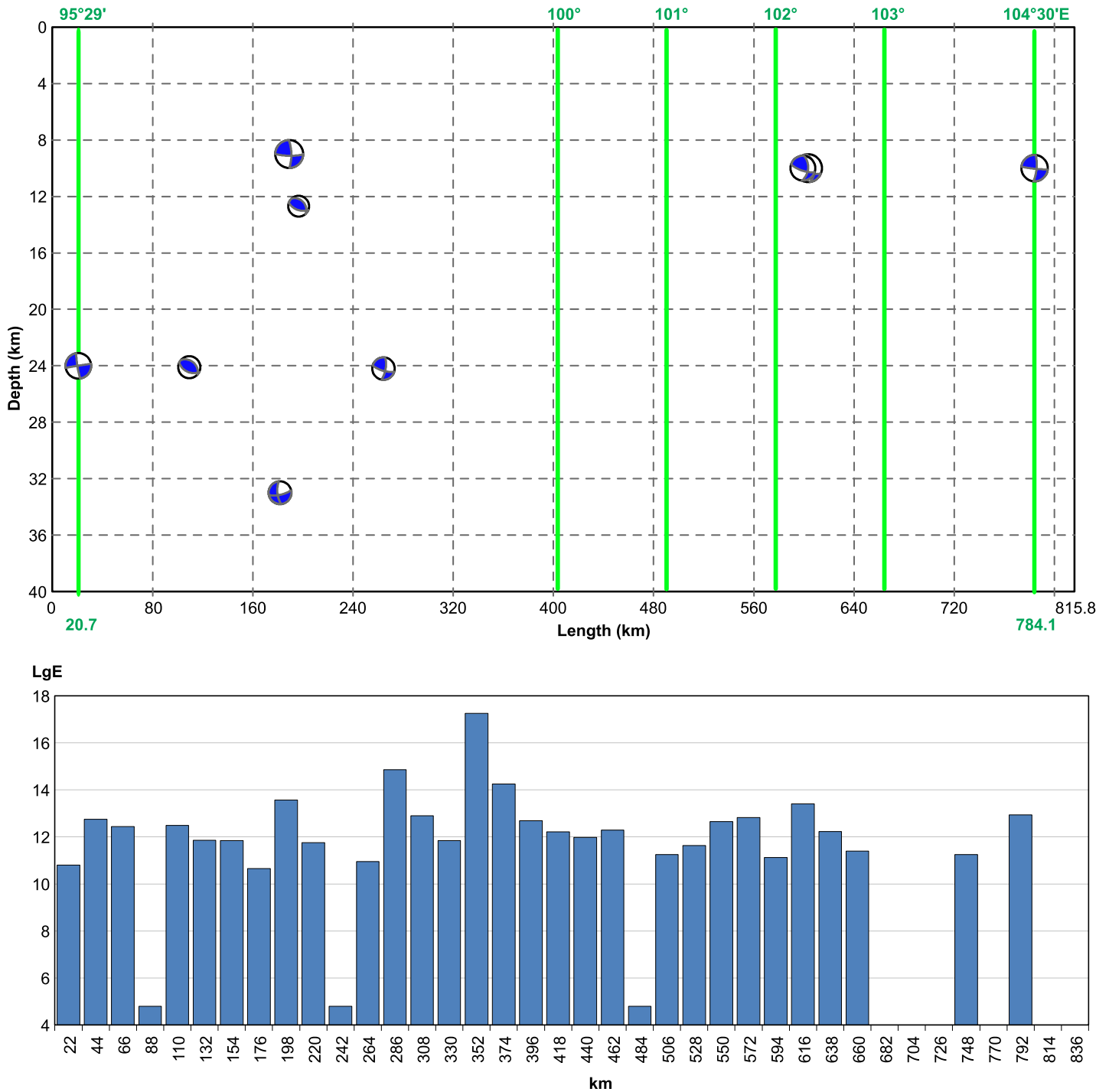
Fig. 3. Top – deep seismic section along Transect 1 across South Gobi and West-Central Mongolia blocks (see Fig. 2) with earthquake mechanisms in hypocenters, based on the CMT data. Bottom – energy dissipation graph along the same transect, based on the NEIC data, at the logarithmic vertical scale. The west here and in other graphs (Figures 4–9) is on the left. Note the sharp energy increase within the geodivider and west of it.

Рис. 3. Наверху – глубинный сейсмический разрез, проходящий вдоль трансекта 1 через блоки Южной Гоби и Западно-Центрально-Монгольский (см. рис. 2) с механизмами землетрясений в гипоцентрах по данным CMT 2017. Внизу – график диссипации сейсмической энергии вдоль того же трансекта по данным NEIC в логарифмическом вертикальном масштабе. Запад здесь и на остальных графиках (рис. 4–9) находится слева. Отмечается резкое возрастание энергии в пределах геодивайдера и к западу от него.

earthquake took place in May 2008 [*Gatinsky et al., 2008*]. This boundary stretches along the large Long-

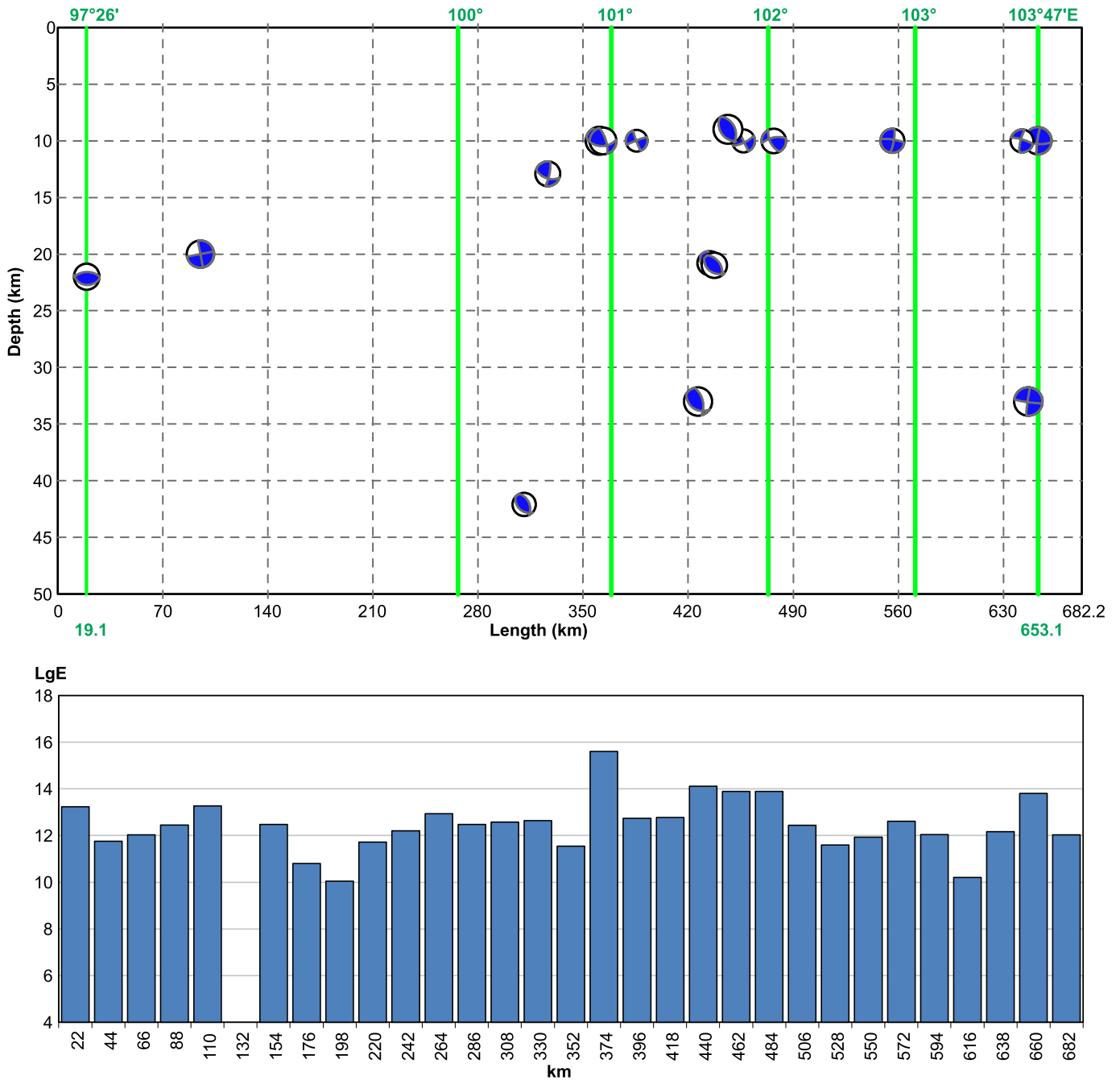men Shan Fault. Thrusting to the SE China Block occurs there, according to geological data [*Xu, Deng, 1996*].

Fig. 4. Deep seismic section and energy dissipation graph along Transect 2 across the boundary of the Jartai and Qilian blocks (see Fig. 2). Note the same tendency of the energy amount increasing within the geodivider and west of it.

Рис. 4. Глубинный сейсмический разрез и график диссипации сейсмической энергии вдоль трансекта 2 через блоки Джартай и Цилян (см. Рис. 2). Отмечается сохранение той же тенденции возрастания объема энергии в пределах геодивайдера и к западу от него.

Field investigations immediately after the earthquake showed a strong horizontal shortening along the NW-dipping rupture with thrusting to SE together with small dextral slipping [*Liu-Zeng et al., 2009*]. In the central segment and a part of the northern segment of the 102–103° geodivider, an increase in the stress intensity is noticeable within the upper crust in the west, and stress decreases to the east [*Heidbach et al., 2016*].

A volume of the total seismic energy releasing at the eastern boundary of the Bayanhar Block comes only to $1.131 \cdot 10^{15}$ J beginning from 1976 without the latest events of 2008. Apparently, this region was in a relative "seismic gap" after the last strong earthquake (M 7.4) that occurred in 1973. The seismic energy accumulated during that period was released by the catastrophic Wenchuan earthquake in May 2008, and amounted to
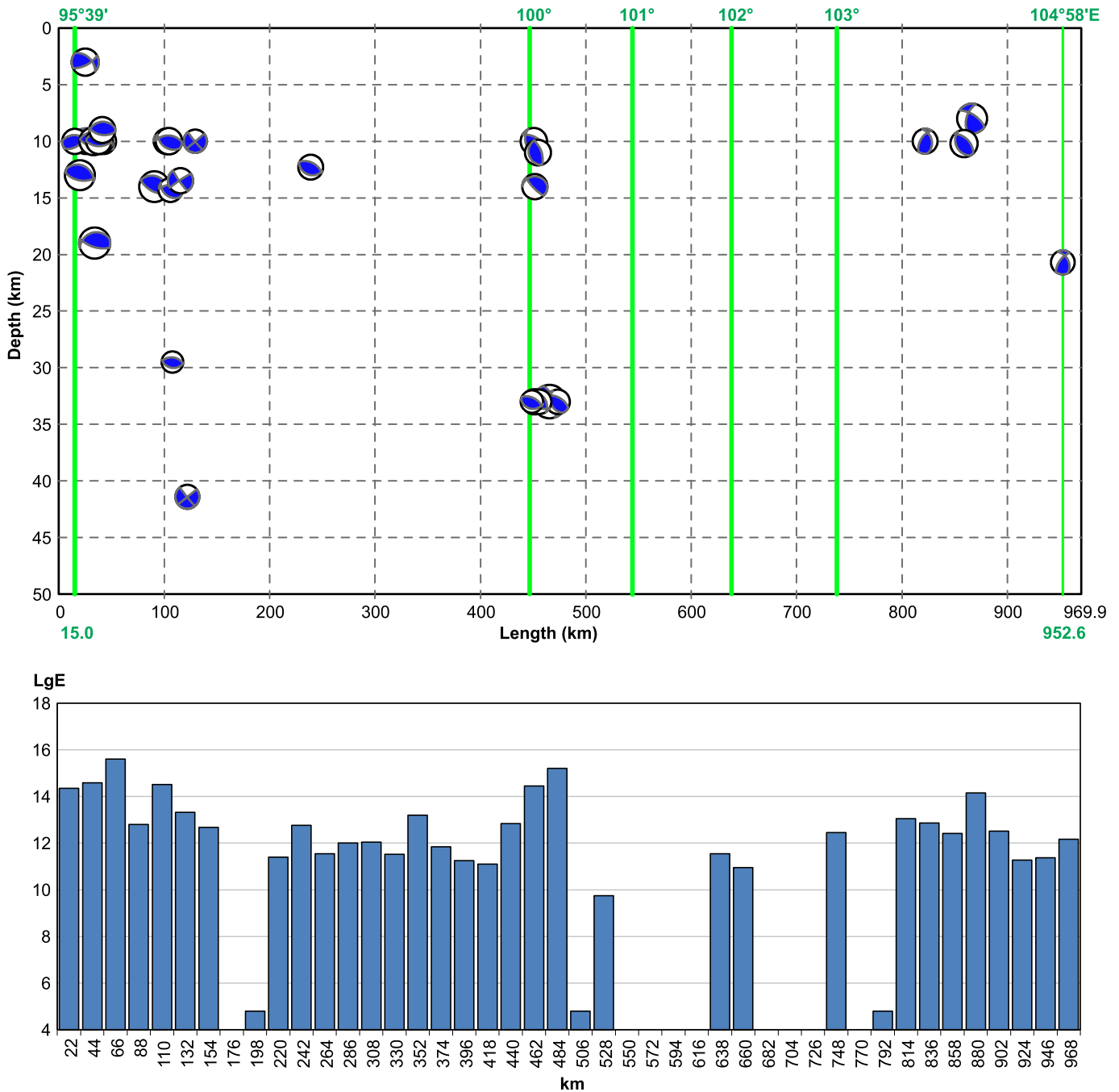
Fig. 5. Deep seismic section and energy dissipation graph along Transect 3 across the West Qinlin and Qaidam blocks (see Fig. 2). The energy volume increases at some distance west of the geodivider.

Рис. 5. Глубинный сейсмический разрез и график диссипации сейсмической энергии вдоль трансекта 3, пересекающего блоки Западный Цинлин и Цайдам (см. рис. 2). Объем энергии возрастает на некотором расстоянии к западу от геодивайдера.

9.251·10^{16} J [*Gatinsky et al., 2011*]. This value is only a little smaller than the energy of the western Pacific subduction zones (11.79–15.33)·10^{16} J [*Gatinsky, Vladova, 2008*]. Computer-simulated GPS vectors confirm the clock-wise rotation of the Bayanhar Block (see Fig. 2). It is likely that only the upper crust is involved in the rotation, because low velocity layers are revealed by seismic tomography data in the eastern half of the Bayanhar Block at the depth of 20–30 km [*Yuan et al., 2000; Sol et al., 2007*]. The SE boundary of the Bayanhar Block coincides with the sharp step in the crust and in the lithosphere along the 102–103° E geodivider, and a significant increase in the lithosphere thickness (up to 130–170 km) is recorded to the east under the Sichuan Basin (compare to the thickness of 100–120 km under East Tibet) [*Hu et al., 2012*].
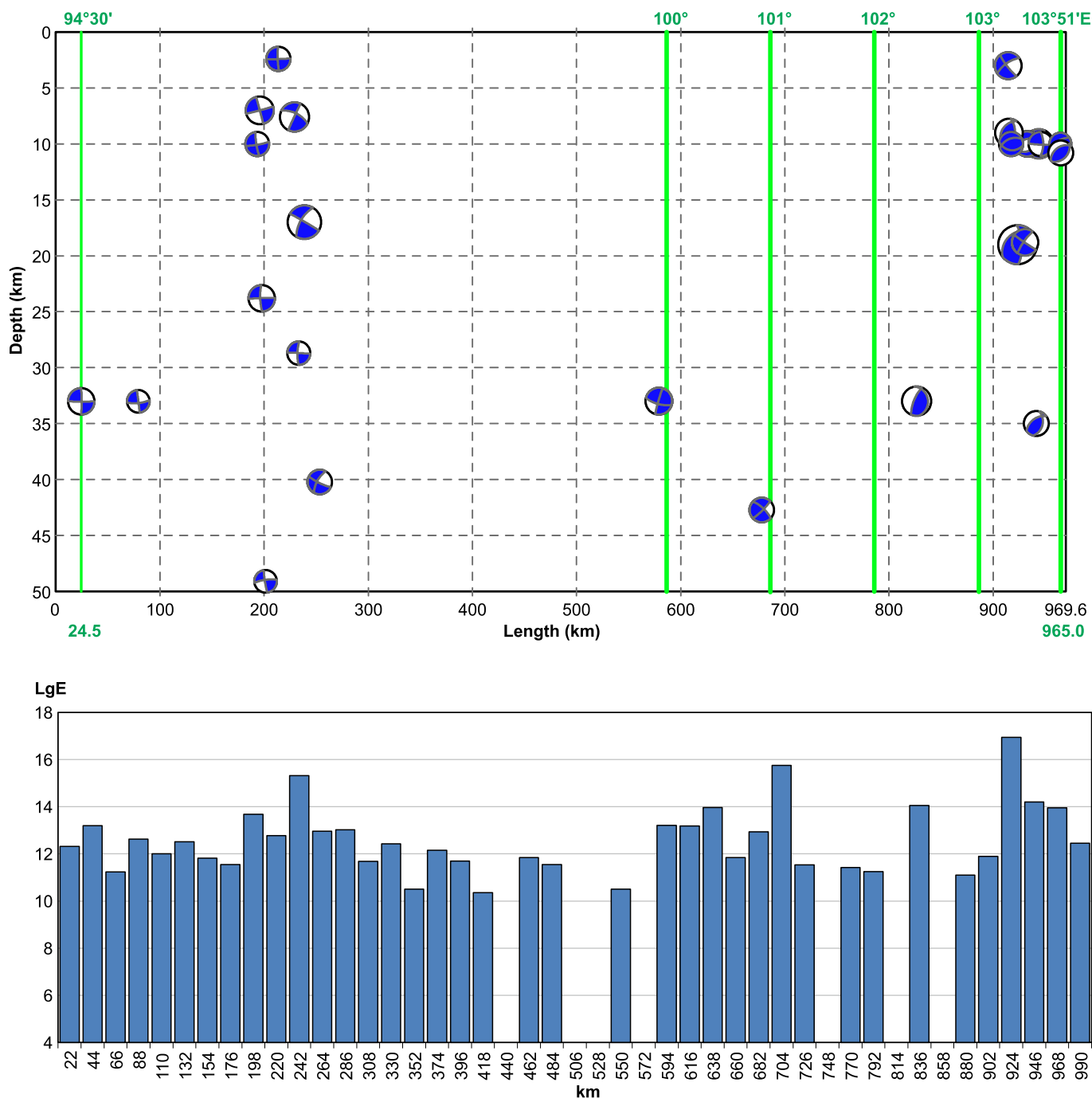
Fig. 6. Deep seismic section and energy dissipation graph along Transect 4 across the Bayanhar Block and its boundary with North Tibet. Note the energy amount increasing at the eastern boundary of the geodivider with the prevalence of the right-lateral slips and thrusts to NW at the depth of 3–43 km at the SE border of the Bayanhar Block near Chengdu where the catastrophic Wenchuan earthquake took place. In the west, along the Bayanhar–Tibet boundary, numerous steady left-lateral slips confirm the displacement direction along the SW block border.

Рис. 6. Глубинный сейсмический разрез и график диссипации сейсмической энергии вдоль трансекта 4 через блок Баянхар и его границу с Северным Тибетом. Объем энергии возрастает на восточной границе геодивайдера с преобладанием правосторонних сдвигов и надвигов к СЗ на глубине 3–43 км на юго-восточной границе блока Баянхар вблизи г. Ченгду, где произошло катастрофическое Венчуанское землетрясение. На западе вдоль границы Баянхар – Тибет многочисленные устойчивые левосторонние сдвиги подтверждают направление смещения вдоль юго-западной границы блока Баянхар.

The geodivider stretches northward across North China and Central Mongolia to the SW termination of Lake Baikal, wherein the M 6.3 Kultuk earthquake took place in 2008 at the boundary between the Amurian
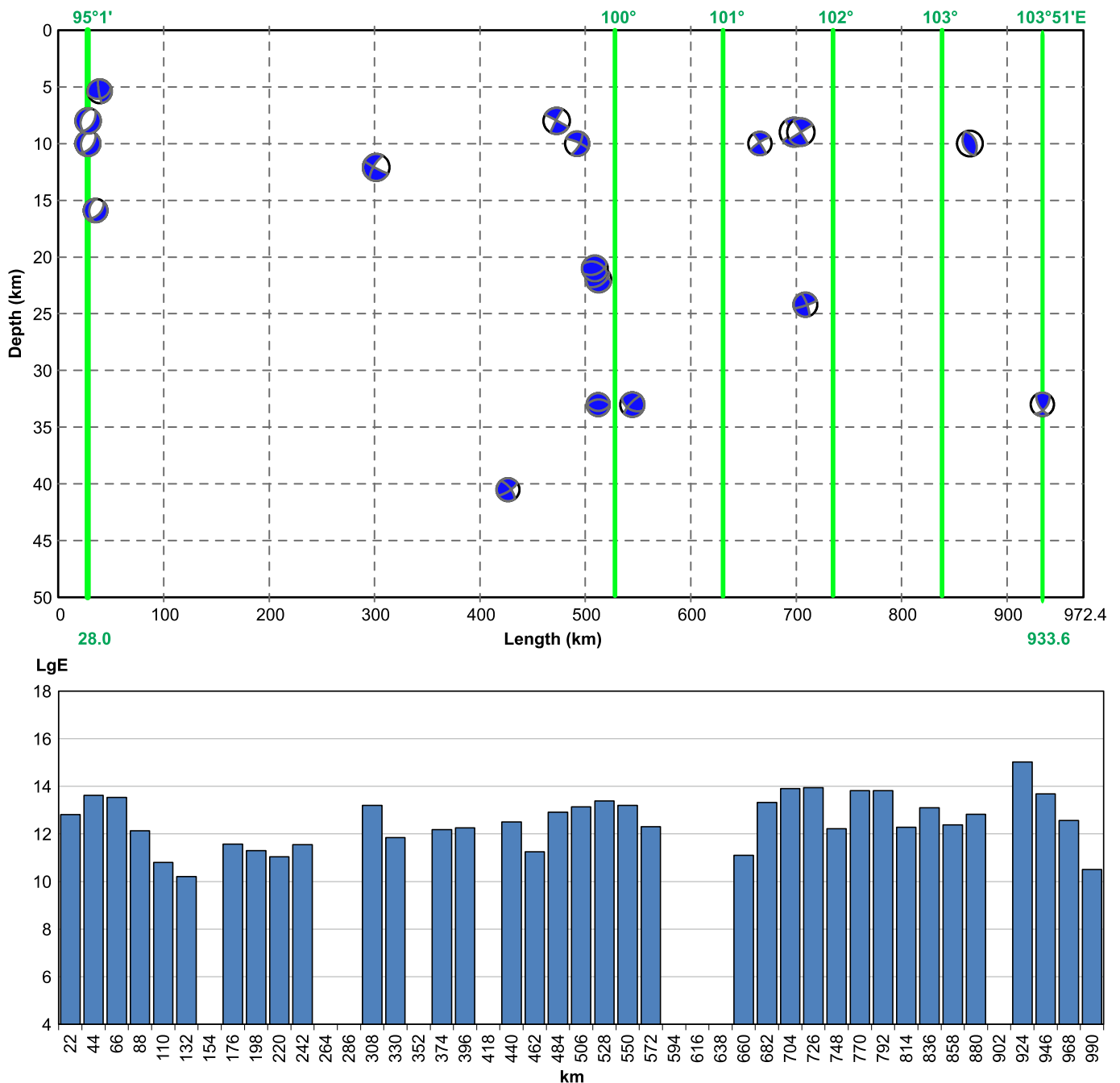
Fig. 7. Deep seismic section and energy dissipation graph along Transect 5 across the SE China, Kam Dian and North Tibet blocks (see Fig. 2). Here the seismic energy amount somewhat decreases within the geodivider and sharply increases west of it, in the region wherein left-lateral and right-lateral slips are dominant. The steady extension at the depth of 5–15 km in the western part of this section is related to local submeridional rifts in Tibet.

Рис. 7. Глубинный сейсмический разрез и график диссипации сейсмической энергии вдоль трансекта 5, пересекающего блоки Юго-Восточного Китая, Кам Диан и Северо-Тибетский (см. рис. 2). Здесь уровень сейсмической энергии частично уменьшается в пределах геодивайдера и резко возрастает к западу от него с преобладанием левосторонних и правосторонних сдвигов. Устойчивое растяжение в западной части разреза на глубине 5–15 км связано с локальными субмеридиональными рифтами в Тибете.

Block and North Eurasian Plate. Irkutsk scientists [*Miroshnichenko et al., 2007*] established the predominant clockwise rotation in this region as evidenced by the data of the local GPS network, showing the vectors changing gradually from NNE to ENE, east and ESE. Such changes of the GPS vector directions are corroborated by the change of tension west and east of southern termination of Lake Baikal.
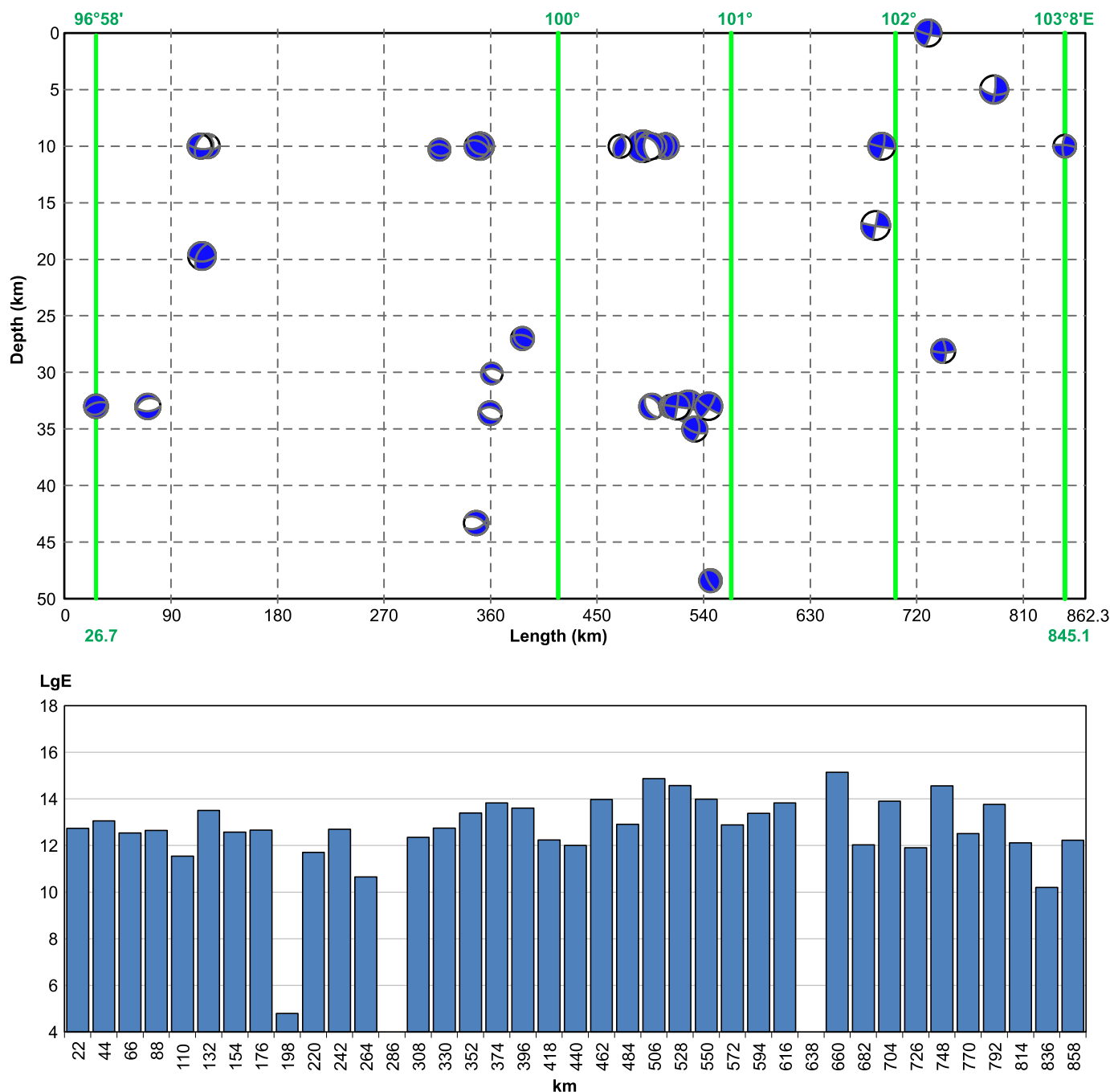
Fig. 8. Deep seismic section and energy dissipation graph along Transect 6 across the southern parts of the same blocks (see Fig. 2). Note left-lateral slips with an increased energy release, which characterizes the geodivider, and many extension structures developing in the west in the North Tibet Block at the depth of 10–44 km.

Рис. 8. Глубинный сейсмический разрез и график диссипации сейсмической энергии вдоль трансекта 6 через южную часть тех же блоков (см. рис. 2). Следует обратить внимание на левосторонние сдвиги с увеличенным высвобождением энергии, которые характеризуют геодивайдер. Многочисленные структуры растяжения развиты западнее в Северо-Тибетском блоке на глубинах 10–44 км.

Transpressive tensions predominate in the western Tunka Trough, wherein left-lateral strike-slips are developed [*Gatinsky et al., 2009; San'kov et al., 2014*]. It should be noted that strike-slips are replaced in the east by later normal faults in the flanks of the Barguzin depression being a part of the Baikal Rift System east of Lake Baikal. The earlier strike-slips caused seismic dislocations displacing thalwegs of the right-lateral tributaries of the Barguzin River. The later normal faults disturbing these strike-slips go through all the rocks from the Paleozoic granite to the Quaternary alluvium.
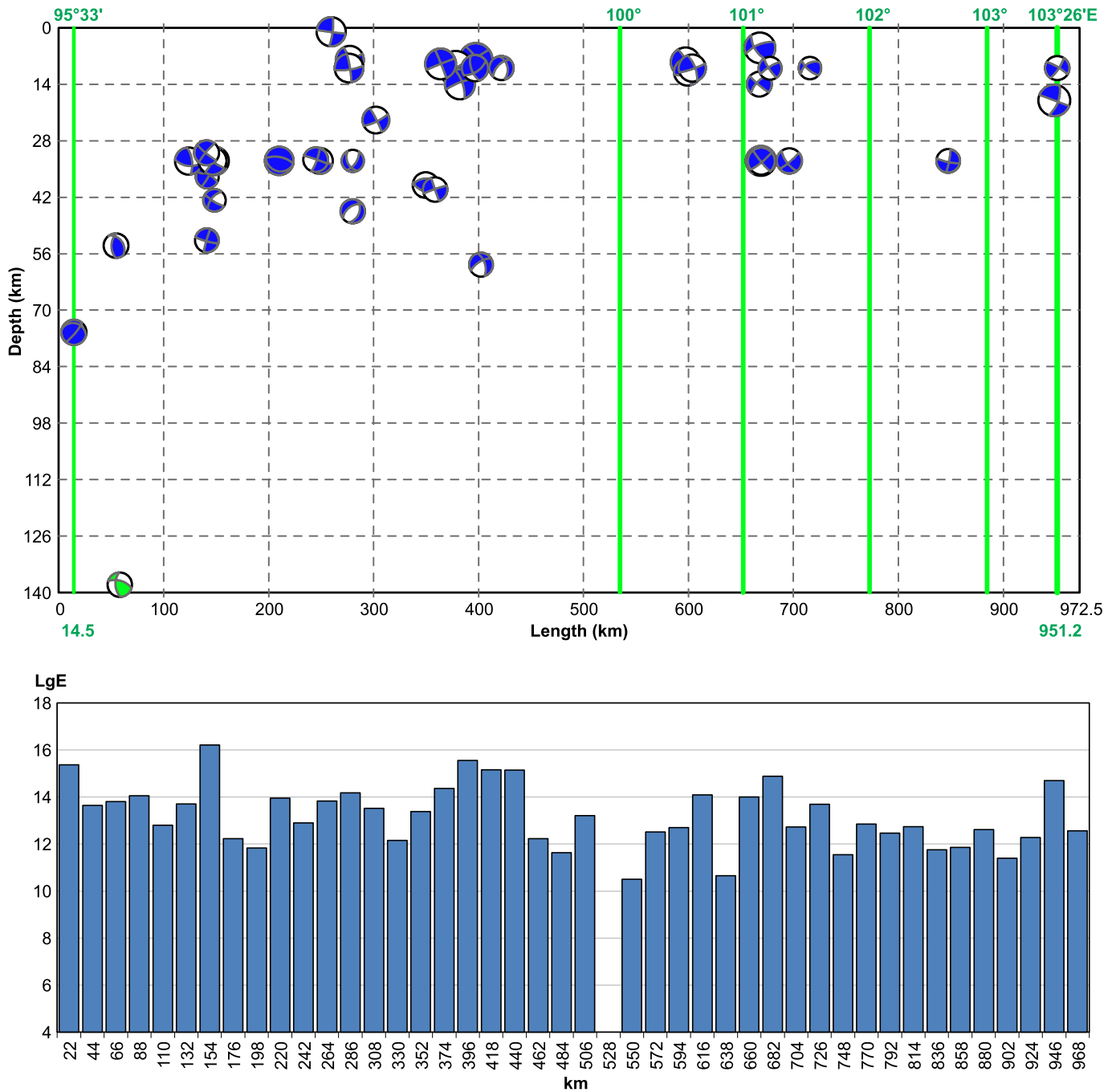
Fig. 9. Deep seismic section and energy dissipation graph along Transect 7 across the Indochina, Shan and West Burma blocks (see Fig. 2). Submeridional and NE slips at the depth of 0–56 km develop within these blocks. In the west of this section, mechanism solutions correspond to the eastern dipping slab of the West Burma subduction zone sinking to the depth of 140 km.

Рис. 9. Глубинный сейсмический разрез и график диссипации сейсмической энергии вдоль трансекта 7, пересекающего блоки Индокитайский, Шан и Западно-Бирманский (см. рис. 2). Субмеридиональные и северо-восточные сдвиги развиты в этих блоках на глубинах 0–56 км. На северо-западе этого трансекта решения механизмов землетрясений отвечают восточному падению слэба Западно-Бирманской зоны субдукции, погружающемуся до 140 км.

7. CONNECTION OF THE GEODIVIDER WITH ANOMALIES IN THE DEEP CRUST AND MANTLE

The 102–103° E geodivider coincides in the first approximation with the boundary between the Central Asian and East Asian transitional zones. Currently, the former is dominated by the transpression tectonic regime with compression due to the Hindustan indenter pressure. In the East Asian Transitional Zone, the transtension regime has developed with modern tension

due to deep submergence [*Parfeevets, San'kov, 2012*] and, probably, gradual disintegration and disappearance of the Pacific subduction slab with depth. Mantle plumes arising under Transbaikalia and East Mongolia [*Gatinsky, Prokhorova, 2014*] also have an influence on the development of the transtension regime.

It is worth noting that an abrupt change in the crust thickness coincides with the central and southern parts of the 102–103° E geodivider. The thickness decreases from 45–70 km in the west to 35–40 km in the east. The scheme of gravitational anomalies in the Bouguer reduction [*Bonvalot et al., 2012*] shows that the geodivider delimits the areas in Central Asia with the predominance of anomalies –100 to –50 mGal in the east and –150 to –200 mGal in the west, corresponding to the increasing crustal thickness values in the same direction. This change in the crustal thickness is observed across this entire region along with abundant basic volcanic rocks, including the Cenozoic basalt in the east.

As concern the whole lithosphere thickness, it does not exceed 60-80 km at the eastern continental margin of Asia, as evidenced by the upper mantle xenoliths. This may result from thinning-out of the lithosphere due to intensive Mesozoic tension processes [*Li et al., 2011; Zhang et al., 2012*]. Tomography data and analysis of the hypocenters depth suggest that the Pacific subduction slab gradates at the depth of about 600 km along the boundary between the upper and lower mantle. It stretches westwards for more than 1500 km approximately up to the 102–103° E geodivider. This results in the lithosphere heating, intracontinental volcanism and formation of tension basins in the East Asian Transitional Zone [*Huang, Zhao, 2009*].

It is of interest to consider also the metallogenic characteristics of the areas surrounding the 102–103°E geodivider. This aspect turns out more intricate than it seems. According to calculations by S. Cherkasov [*Gatinsky et al., 2005*], the ore deposits of the lithophylic type predominate in the western domain of the Eurasian lithosphere (wherein the crust is thicker), whereas the chalcophylic type of mineralization is observed in the eastern domain. In the 102–103° geodivider itself, the concentration of small- to large-size ore deposits is one and a half times higher than that in the western and eastern domains, and iron, lead-zinc and copper deposits are relatively abundant in comparison with the side parts (ten, five and four times higher concentrations, respectively). Another feature of the geodivider is a total absence of tin, antimony, tungsten and mercury deposits.

Therefore, the 102–103° zone indeed divides two large domains of the Eurasian lithosphere: the western one having the thick crust and sufficiently lithophylic type of metallogeny, and the eastern domain having the thinner crust and mainly chalcophylic type of minerali-

zation. It is, of course, only the principal scheme and some exceptions exist. There are several blocks with rather old pre-Cambrian crust in the eastern domain, wherein the lithophylic tendency somewhat increases. Among them, we can mention the major part of the Yangtze platform with the well-known tin-bearing Getzu deposit and Cathaysia in South East China with numerous tin, tungsten and molybdenum deposits. But, even in these cases an admixture of chalcophylic elements is rather high.

Genetically, such differences can be related not only to the latest plate interaction in the Eastern Eurasia, which is obvious, but may also be connected with a more profound heterogeneity of the Earth material. This conclusion is supported by the following data. The 102–103° E geodivider coincides with one of the areas with the highest temperature in the upper mantle at least at the depth of 150 km [*Artemjev et al., 1994*]. According to the tomography data from [*Wu et al., 1997; Kozhevnikov, Yanovskaya, 2005*], this zone is marked by some changes in the tomographic features at the depth of 220–400 km. The analysis of anisotropic characteristics under the geodivider, that is named the North-South Tectonic Belt (NSTB) in the Chinese geophysical literature, has shown that lithosphere deformation plays a major role in the observed anisotropy in the north of it, and the lithosphere in this zone is currently subjected to vertically coherent deformation [*Chang et al., 2015*]. In the southern part of NSTB, the observed anisotropy seems connected with the asthenosphere mantle flow beneath the thin lithosphere. The subduction and rollback/retreat of the Burma-Sunda slabs generate a SE-trending flow, which produces a differential flow between the lithosphere and sub-asthenosphere. The differential shear is sufficient to generate the observed anisotropy in the southern part of the zone.

8. DISCUSSION AND CONCLUSION

The direction of the *P*- and *S*-waves anisotropy shows coupling deformations in the lithosphere, upper mantle and crust within the great part of Central Asia [*San'kov et al., 2011*]. At the same time, different vectors of horizontal displacement in the crust and mantle east of the East Himalayan Syntax and along of the southern part of the 102–103° geodivider indicate decoupling of these layers under the influence of the Hindustan-Asia collision [*Hu et al., 2012*]. The thinner lithosphere of the eastern Tibet undergoes heating and delaminating under the influence of the flow from the underlying hot asthenosphere, which is branching into the northeastward and southeastward flows due to the resistance of the cold and rigid Sichuan Basin lithosphere. The eastward extrusion of the Tibet lithosphere was assumed for the first time in [*Molnar, Tapponier,*

1975]. The Tibet lithosphere delamination causes its fragmentation during the interaction with the rigid and cold SE Asia Block. The GPS data shows the intensive clock-wise turning of the crust within the Bayan Har, Kam Dian, Shan and SE China blocks. The lithosphere dynamic model suggests that the Yunnan and Indochina crust is moving in the SE- and southward direction with respect to the mantle, while the mantle is displacing to NE. At the same time, beneath the more western part of Tibet, both the crust and the mantle move northward [*Flesch et al., 2005; Sol et al., 2007*].

The GPS vectors east of the geodivider mainly have the direction of 106–121° SE [*Lukhnev et al., 2010*] with velocities of 26–35 mm/y (see Fig. 2). West of it, predominant are the vectors to the north and northeast with velocities from 50 to 23–25 mm/y. Some researchers suppose that changes in the vectors are related to the crust layering and layers rolling-down from the high Tibet Plateau [*Copley, 2008*]. This assumption is indirectly supported by the INDEPTH seismic and magnetotelluric sounding data [*Li et al., 2003; Solon et al., 2005*]. According to the INDEPTH data, there are layers of increased plasticity and partial melting of rocks in the Tibet crust at the depth of 25–40 km. A sharp increase of the upper crust thickness east of the 102–103° geodivider in the SE China Block can be due to the fact that the upper crust is tearing away and moving independently eastwards along the more plastic middle and low crust [*Shen et al., 2005; Zhang et al., 2009; Li et al., 2011*].

Therefore, the 102–103° E geodivider is as a kind of a large regional geological-geophysical border. It may be compared with such structures as the Tornquist Line, and, by its scale, with the Uralian and Appalachian fronts and some others large structures. This zone appears at the trans-Eurasian Global Geoscience Transect 21 as a gigantic step in the crust and the whole lithosphere [*Yuan et al., 2000*].

9. ACKNOWLEDGEMENT

10. REFERENCES

Artemjev M.E., Kaban M.K., Kucherinenko V.A., Demjanov G.V., Taranov V.A., 1994. Subcrustal density inhomogeneities of Northern Eurasia as derived from the gravity data and isostatic models of the lithosphere. *Tectonophysics* 240 (1–4), 248–280. https://doi.org/10.1016/0040-1951(94)90275-5.

Bonvalot S., Balmino G., Briais A., Kuhn M., Peyrefitte A., Vales N., Biancale R., Gabalda G., Moreaux G., Reinquin F., Sarrailh M., 2012. World Gravity Map. Scale 1:50000000. BGI-CGMW-CNES-IRD, Paris.

Chang L.-J., Ding Z.-F., Wang Ch.-Yo., 2015. Upper mantle anisotropy beneath the southern segment of North-South tectonic belt, China. *Chinese Journal of Geophysics – Chinese Edition* 58 (11), 4052–4067.

Copley A., 2008. Kinematics and dynamics of the southeastern margin of the tibetan plateau. *Geophysical Journal International* 174 (3), 1081–1100. https://doi.org/10.1111/j.1365-246X.2008.03853.x.

Flesch L.M., Holt W.E., Silver P.G., Stephenson M., Wang Ch.-Yo., Chan W., 2005. Constraining the extent of crust-mantle coupling in Central Asia using GPS, geologic, and shear wave splitting data. *Earth and Planetary Science Letters* 238 (1–2), 248–268. https://doi.org/10.1016/j.epsl.2005.06.023.

Gatinsky Y.G., 2005. Tectonics and geodynamic prerequisites of mineral resource distribution in the Indochina Region. *Geology of Ore Deposits* 47 (4), 309–325.

Gatinsky Y.G., Prokhorova T.V., 2014. Superficial and deep structure of Central Asia as example of continental lithosphere heterogeneity. *Universal Journal of Geoscience* 2 (2), 43–52. https://doi.org/10.13189/ujg.2014.020202.

Gatinsky Y.G., Prokhorova T.V., Rundquist D.V., Vladova G.L., 2009. Zones of catastrophic earthquakes of Central Asia: geodynamics and seismic energy. *Russian Journal of Earth Sciences* 11 (1), ES1001. https://doi.org/10.2205/2009ES000326.

Gatinsky Y.G., Rundquist D.V., Cherkasov S.V., 2005. Geodivider of 102–103° in East Asia: geological and metallogenic signs. In: Tectonics of Earth crust and mantle. tectonic regularities of minerals placing. Proceedings of the 28th Tectonic Conference. GEOS, Moscow, p. 127–130 (in Russian). [*Гатинский Ю.Г., Рундквист Д.В., Черкасов С.В.* Геораздел 102–103° на востоке Азии: геологические и металлогенические признаки // Тектоника земной коры и мантии. Тектонические закономерности размещения полезных ископаемых: Материалы 28-го Тектонического совещания. М.: ГЕОС, 2005. С. 127–130].

Gatinsky Y.G., Rundquist D.V., Vladova G.L., Prokhorova T.V., 2008. Geodynamics of the Sichuan earthquake region in May 12, 2008. *Doklady Earth Sciences* 423A (9), 1507–1509. https://doi.org/10.1134/S1028334X08090419.

Gatinsky Y.G., Rundquist D.V., Vladova G.L., Prokhorova T.V., 2011. Up-to-date geodynamics and seismicity of Central Asia. *International Journal of Geosciences* 2, 1–12. https://doi.org/10.4236/ijg.2011.21001.

Gatinsky Y.G., Vladova G.L., 2008. Subduction zones of SE Asia: main types, seismicity and mineralization. In: Proceedings of the VAG International Symposium (November 7–9, 2008, Hanoi, Vietnam). Special issue of *Journal of Geology*: International Year of Planet Earth, p. 9–16. Available from: http://idm.gov.vn/nguon_luc/Xuat_ban/2008/b31-32/b9.htm.

Heidbach O., Rajabi M., Reiter K., Ziegler M., WSM Team, 2016. World Stress Map Database. Release 2016. GFZ Data Services. https://doi.org/10.5880/WSM.2016.001.

Hu J., Yang H., Xu X., Wen L., Li G., 2012. Lithospheric structure and crust – mantle decoupling in the southeast edge of the Tibetan Plateau. *Gondwana Research* 22 (3–4), 1060–1067. https://doi.org/10.1016/j.gr.2012.01.003.

Huang J., Zhao D., 2009. Seismic imaging of the crust and upper mantle under Beijing and surrounding regions. *Physics of the Earth and Planetary Interiors* 173 (3–4), 330–348. https://doi.org/10.1016/j.pepi.2009.01.015.

Kanamori H., Anderson D.L., 1975. Theoretical basis of some empirical relations in seismology. *Bulletin of the Seismological Society of America* 65 (5), 1073–1095.

Komarov Yu.V., Belichenko V.G., Misharina L.A., Petrov P.A., 1978. Verkhoyansk-Burma zone of Central and East Asia structures joining (VEBIRS Zone). In: Transasian continental VEBIRS zone (Operational Information). East Siberian Branch of Siberian Department, the USSR Academy of Sciences, Irkutsk, p. 5–24 (in Russian) [*Комаров Ю.В., Беличенко В.Г., Мишарина Л.А., Петров П.А.* Верхояно-Бирманская зона сочленения Центрально- и Восточноазиатских структур (зона ВЕБИРС) // Трансазиатская континентальная зона ВЕБИРС (оперативная информация). Иркутск: Восточно-Сибирский филиал СО АН СССР, 1978. С. 5–24].

Kozhevnikov V.M., Yanovskaya T.B., 2005. S-wave velocities distribution in the lithosphere of the Asian continent after data of surface Rayleigh waves. In: K.G. Levi, S.I. Sherman (Eds.), Actual problems of modern geodynamics of Central Asia. Publishing House of SB RAS, Novosibirsk, p. 46–64 (in Russian) [*Кожевников В.М., ЯновскаяТ.Б.* Распределение скоростей S-волн в литосфере Азиатского континента по данным поверхностных волн Релея // Актуальные проблемы геодинамики Центральной Азии / Ред. К.Г. Леви, С.И. Шерман. Новосибирск: Изд-во СО РАН, 2005. С. 46–64].

Li S., Unsworth M.J., Booker J.R., Wei W., Tan H., Jones S., 2003. Partial melt or aqueous fluid in the mid-crust of Southern Tibet? Constraints from INDEPTH magnetotelluric data. *Geophysical Journal International* 153 (2), 289–304. https://doi.org/10.1046/j.1365-246X.2003.01850.x.

Li J., Wang X., Niu F., 2011. Seismic anisotropy and implication for mantle deformation beneath the NE margin of the Tibet plateau and Ordos plateau. *Physics of the Earth and Planetary Interiors* 189 (3–4), 157–170. https://doi.org/10.1016/j.pepi.2011.08.009.

Liu-Zeng J., Zhang Z., Wen L., Tapponnier P., Sun J., Xing X., Hu G., Xu Q., Zeng L., Ding L., 2009. Co-seismic ruptures of the 12 May 2008, Ms 8.0 Wenchuan earthquake, Sichuan: east–west crustal shortening on oblique, parallel thrusts along the eastern edge of Tibet. *Earth and Planetary Science Letters* 286 (3–4), 355–370. https://doi.org/10.1016/j.epsl.2009.07.017.

Lukhnev A.V., San'kov V.A., Miroshnichenko A.I., Ashurkov S.V., Calais E., 2010. GPS rotation and strain rates in the Baikal–Mongolia region. *Russian Geology and Geophysics* 51 (7), 785–793. https://doi.org/10.1016/j.rgg.2010.06.006.

Miroshnichenko A.I., San'kov V.A., Parfeevets A.V., Lukhnev A.V., 2007. State of stress and strain of the Earth crust of the basins of North Mongolia from the model results. In: Proceedings of the conference commemorating the 50th anniversary of the 1957 Gobi-Altay earthquake. Ulaanbaatar–Irkutsk, p. 138–143.

Molnar P., Tapponier P., 1975. Cenozoic tectonics of Asia: effects of a continental collision. *Science* 189 (4201), 419–426. https://doi.org/10.1126/science.189.4201.419.

Parfeevets A.V., San'kov V.A., 2012. Late Cenozoic tectonic stress fields of the Mongolian microplate. *Comptes Rendus Geoscience* 344 (3–4), 227–238. https://doi.org/10.1016/j.crte.2011.09.009.

Rundquist D.V., Gatinsky Yu.G., Cherkasov S.V., 2004. The natural trans-Eurasian divider: structural and metallogenic evidences. In: Abstracts volume of the 32nd International Geological Congress. Part 2. Florence, Italy, p. 620.

San'kov V.A., Lukhnev A.V., Miroshnichenko A.I., Dobrynina A.A., Ashurkov S.V., Byzov L.M., Dembelov M.G., Calais E., Déverchère J., 2014. Contemporary horizontal movements and seismicity of the South Baikal Basin (Baikal rift system). *Izvestiya, Physics of the Solid Earth* 50 (6), 785–794. https://doi.org/10.1134/S106935131406007X.

San'kov V.A., Parfeevets A.V., Lukhnev A.V., Miroshnichenko A.I., Ashurkov S.V., 2011. Late Cenozoic geodynamics and mechanical coupling of crustal and mantle deformation in Mongolia-Siberia mobile area. *Geotectonics* 45 (5), 378–393. https://doi.org/10.1134/S0016852111050049.

San'kov V.A., Parfeevets A.V., Miroshnichenko A.I., Sankov A.V., Bayasgalan A., Battogtokh D., 2015. Active faults paragenesis and the state of crustal stresses in the Late Cenozoic in Central Mongolia. *Geodynamics & Tectonophysics* 6 (4), 491–518 (in Russian) [*Саньков В.А., Парфеевец А.В., Мирошниченко А.И., Саньков А.В., Баясгалан А., Баттогтох Д.* Парагенез активных разломов и позднекайнозойское напряженное состояние земной коры центральной части Монголии // *Геодинамика и тектонофизика* 6 (4), 491–518]. https://doi.org/10.5800/GT-2015-6-4-0191.

Seminskii K.Zh., 2008. Hierarchy in the zone block lithospheric structure of Central and Eastern Asia. *Russian Geology and Geophysics* 49 (10), 771–779. https://doi.org/10.1016/j.rgg.2007.11.017.

Shen Z.K., Lü J., Wang M., Bürgmann R., 2005. Contemporary crustal deformation around the southeast borderland of the Tibetan plateau. *Journal of Geophysical Research: Solid Earth* 110 (B11), B11409. https://doi.org/10.1029/2004JB003421.

Sherman S.I., 2012. Destruction of the lithosphere: Fault block divisibility and its tectonophysical regularities. *Geodynamics & Tectonophysics* 3 (4), 315–344 (in Russian) [*Шерман С.И.* Деструкция литосферы: разломно-блоковая делимость и ее тектонофизические закономерности // *Геодинамика и тектонофизика.* 2012. Т. 3. № 4. С. 315–344]. https://doi.org/10.5800/GT-2012-3-4-0077.

Sherman S.I., 2015. Localization of recent strong earthquakes in Central Asia: a rare combination of geodynamic and trigger factors. In: V.V. Adushkin, G.G. Kocharian (Eds.), Trigger effects in geosystems. GEOS, Moscow, p. 138–149 (in Russian) [*Шерман С.И.* Локализация современных сильных землетрясений в Центральной Азии: редкое сочетание геодинамических и триггерных факторов // Триггерные эффекты в геосистемах / Ред. В.В. Адушкин, Г.Г. Кочарян. М.: ГЕОС, 2015. С. 138–149].

Sherman S.I., 2016. Tectonophysical signs of the formation of strong earthquake foci in seismic zones of Central Asia. *Geodynamics & Tectonophysics* 7 (4), 495–512 (in Russian) [*Шерман С.И.* Тектонофизические признаки формирования очагов сильных землетрясений в сейсмических зонах Центральной Азии // *Геодинамика и тектонофизика.* 2016. Т. 7. № 4. С. 495–512]. http://doi.org/10.5800/GT-2016-7-4-0219.

Sherman S.I., Seminsky K.Zh., Cheremnykh A.V., 1999. Destructive zones and fault-produced block structures of Central Asia. *Tikhookeanskaya Geologiya* 18 (2), 41–53 (in Russian) [*Шерман С.И., Семинский К.Ж., Черемных А.В.* Деструктивные зоны и разломно-блоковые структуры Центральной Азии // *Тихоокеанская геология.* 1999. Т. 18. № 2. С. 41–53].

Sol S., Meltze A., Bürgmann R., van der Hilst R.D., King R., Chen Z., Koons P.O., Lev E., Liu Y.P., Zeitler P.K., Zhang X., Zhang J., Zurek B., 2007. Geodynamics of the southeastern Tibetan plateau from seismic anisotropy and geodesy. *Geology* 35 (6), 563–566. https://doi.org/10.1130/G23408A.1.

Solon K.D., Jones A.G., Nelson K.D., Unsworth M.J., Kidd W.F., Wei W., Tan H., Jin S., Deng M., Booker J.R., Li S., Bedrosian P., 2005. Structure of the crust in the vicinity of the Banggong-Nujiang Suture in Central Tibet from INDEPTH magnetotelluric data. *Journal of Geophysical Research: Solid Earth* 110 (B10), B10102. https://doi.org/10.1029/2003JB002405.

Tectonic Map of China and Adjacent Regions, 1999. Compiled by the Tectonic Division of the Institute of Geology, Chinese Academy of Geological Sciences. Chief compiler Ren Jishun. 1st ed. Geological Publishing House, Beijing.

Trifonov V.G., Soboleva O.V., Trifonov R.V., Vostrikov G.A., 2002. Recent Geodynamics of the Alpine-Himalayan Collision Belt. GEOS, Moscow, 225 p. (in Russian) [*Трифонов В.Г., Соболева О.В., Трифонов Р.В., Востриков Г.А.* Современная геодинамика Альпийско-Гималайского коллизионного пояса. М.: ГЕОС, 2002. 225 с.].

Wang Ch.Yo., Yang W.C., Wu J.P., Ding Zh.F., 2015. Study on the lithospheric structure and earthquakes in North-South Tectonic Belt. *Chinese Journal of Geophysics – Chinese Edition* 58 (11), 3867–3901.

Wu F.T., Levshin A.L., Kozhevnikov V.M., 1997. Rayleigh wave group velocity tomography of Siberia, China and the vicinity. *Pure and Applied Geophysics* 149 (3), 447–473. https://doi.org/10.1007/s000240050035.

Xu X., Deng Q., 1996. Nonlinear characteristics of paleoseismicity in China. *Journal of Geophysical Research: Solid Earth* 101 (B3), 6209–6231. https://doi.org/10.1029/95JB01238.

Yuan X., Egorov A.S., GEMOC, 2000. A Short Introduction to Global Geoscience Transect 21: Arctic Ocean – Eurasia–Pacific Ocean. Science Press, 32 p.

Zhang Zh., Bai Zh., Mooney W., Wang C., Chen X., Wang E., Teng J., Okaya J., 2009. Crustal structure across the Three Gorges area of the Yangtze platform, Central China, from seismic refraction/wide-angle reflection data. *Tectonophysics* 475 (3–4), 423–437. https://doi.org/10.1016/j.tecto.2009.05.022.

Zhang Zh., Wu J., Deng Ya., Teng J., Zhang X., Chen Yu., Panza G., 2012. Lateral variation of the strength of lithosphere across the eastern North China Craton: New constraints on lithospheric disruption. *Gondwana Research* 22 (3–4), 1047–1059. https://doi.org/10.1016/j.gr.2012.03.006.

Zonenshain L. P., Savostin L. A., 1981. Geodynamics of the Baikal rift zone and plate tectonics of Asia. *Tectonophysics* 76 (1–2), 1–45. https://doi.org/10.1016/0040-1951(81)90251-1.

Yuri G. Gatinsky, Doctor of Geology and Mineralogy
V.I. Vernadsky State Geological Museum of RAS
11 Mokhovaya street, building 11, Moscow 125009, Russia

✉ e-mail: gatinsky@gmail.com
ORCID ID https://orcid.org/0000-0001-7225-7073

Юрий Георгиевич Гатинский, докт. геол.-мин. наук
Государственный геологический музей им. В.И. Вернадского РАН
125009, Москва, ул. Моховая, 11, стр. 11, Россия

Tatiana V. Prokhorova
Institute of Earthquake Prediction Theory and Mathematical Geophysics of RAS
84/32 Profsoyuznaya street, Moscow 117997, Russia

e-mail: tatprokh@mitp.ru

Татьяна Викторовна Прохорова
Институт теории прогноза землетрясений и математической геофизики РАН
117997, Москва, ул. Профсоюзная, 84/32, Россия

Dmitriy V. Rundquist, Doctor of Geology and Mineralogy, Academician of RAS
V.I. Vernadsky State Geological Museum of RAS
11 Mokhovaya street, building 11, Moscow 125009, Russia

e-mail: dvr@sgm.ru
ORCID ID https://orcid.org/0000-0001-8428-5936

Дмитрий Васильевич Рундквист, докт. геол.-мин. наук, академик РАН
Государственный геологический музей им. В.И. Вернадского РАН
125009, Москва, ул. Моховая, 11, стр. 11, Россия